



THE UNIVERSITY *of* EDINBURGH

Edinburgh Research Explorer

Reduction of Ice Adhesion on Nanostructured and Nanoscale Slippery Surfaces

Citation for published version:

Haworth, L, Yang, D, Agrawal, P, Torun, H, Hou, X, McHale, G & Fu, R 2023, 'Reduction of Ice Adhesion on Nanostructured and Nanoscale Slippery Surfaces', *Nanotechnology and Precision Engineering*, vol. 6, no. 1, 013007. <https://doi.org/10.1063/10.0017254>

Digital Object Identifier (DOI):

[10.1063/10.0017254](https://doi.org/10.1063/10.0017254)

Link:

[Link to publication record in Edinburgh Research Explorer](#)

Document Version:

Publisher's PDF, also known as Version of record

Published In:

Nanotechnology and Precision Engineering

General rights

Copyright for the publications made accessible via the Edinburgh Research Explorer is retained by the author(s) and / or other copyright owners and it is a condition of accessing these publications that users recognise and abide by the legal requirements associated with these rights.

Take down policy



The University of Edinburgh has made every reasonable effort to ensure that Edinburgh Research Explorer content complies with UK legislation. If you believe that the public display of this file breaches copyright please contact openaccess@ed.ac.uk providing details, and we will remove access to the work immediately and investigate your claim.



Reduction of ice adhesion on nanostructured and nanoscale slippery surfaces

Cite as: Nanotechnol. Precis. Eng. 6, 013007 (2023); <https://doi.org/10.1063/10.0017254>

Submitted: 08 December 2022 • Accepted: 29 January 2023 • Published Online: 17 February 2023

 Luke Haworth, Deyu Yang,  Prashant Agrawal, et al.



View Online



Export Citation

ARTICLES YOU MAY BE INTERESTED IN

[The importance of laser wavelength for driving inertial confinement fusion targets. II. Target design](#)

Physics of Plasmas **30**, 012702 (2023); <https://doi.org/10.1063/5.0118093>

[A guide to small fluorescent probes for single-molecule biophysics](#)

Chemical Physics Reviews **4**, 011302 (2023); <https://doi.org/10.1063/5.0131663>

[Local sampling of the SU\(1,1\) Wigner function](#)

AVS Quantum Science **5**, 014404 (2023); <https://doi.org/10.1116/5.0134784>



AIP Advances
Nanoscience Collection

READ NOW!

Reduction of ice adhesion on nanostructured and nanoscale slippery surfaces

Cite as: Nano. Prec. Eng. 6, 013007 (2023); doi: 10.1063/10.0017254

Submitted: 8 December 2022 • Accepted: 29 January 2023 •

Published Online: 17 February 2023



View Online



Export Citation



CrossMark

Luke Haworth,¹  Deyu Yang,² Prashant Agrawal,¹  Hamdi Torun,¹  Xianghui Hou,²
Glen McHale,³  and Yongqing Fu^{1,a)} 

AFFILIATIONS

¹ Faculty of Engineering and Environment, University of Northumbria, Newcastle upon Tyne NE1 8ST, United Kingdom

² State Key Laboratory of Solidification Processing, Shaanxi Key Laboratory of Fiber Reinforced Light Composite Materials, Northwestern Polytechnical University, Xi'an 710072, China

³ Institute for Multiscale Thermofluids, School of Engineering, University of Edinburgh, King's Buildings, Edinburgh EH9 3FB, United Kingdom

^{a)} Author to whom correspondence should be addressed: richard.fu@northumbria.ac.uk

ABSTRACT

Ice nucleation and accretion on structural surfaces are sources of major safety and operational concerns in many industries including aviation and renewable energy. Common methods for tackling these are active ones such as heating, ultrasound, and chemicals or passive ones such as surface coatings. In this study, we explored the ice adhesion properties of slippery coated substrates by measuring the shear forces required to remove a glaze ice block on the coated substrates. Among the studied nanostructured and nanoscale surfaces [i.e., a superhydrophobic coating, a fluoropolymer coating, and a polydimethylsiloxane (PDMS) chain coating], the slippery omniphobic covalently attached liquid (SOCAL) surface with its flexible polymer brushes and liquid-like structure significantly reduced the ice adhesion on both glass and silicon surfaces. Further studies of the SOCAL coating on roughened substrates also demonstrated its low ice adhesion. The reduction in ice adhesion is attributed to the flexible nature of the brush-like structures of PDMS chains, allowing ice to detach easily.

© 2023 Author(s). All article content, except where otherwise noted, is licensed under a Creative Commons Attribution (CC BY) license (<http://creativecommons.org/licenses/by/4.0/>). <https://doi.org/10.1063/10.0017254>

KEYWORDS

Hydrophobic, Superhydrophobic, Polymer surface, Ice adhesion, Wettability, SOCAL

Ice accretion and adhesion have damaging impacts on many sectors, including aviation, renewable energy, and telecommunications.^{1–4} For example, ice formation on aircraft wings poses a great hazard to health and safety; according to the Air Safety Foundation of the Aircraft Owners and Pilots Association, between 1990 and 2000 there were 105 accidents involving fatalities due to the effects of icing.⁵ Renewable energy generation is a key growing area to reduce the amount of energy generated from fossil fuels, but considering the impact that cold weather can have on wind turbines, ice formation can result in power loss, mechanical and electrical failures, and safety issues.⁶ Common passive approaches to tackling this issue have involved either simply painting surfaces or using more-complex icephobic treatments.^{7–9} There have been extensive studies of icephobic coatings for passively preventing

ice accretion and reducing ice adhesion on surfaces; the simplest passive coating is a black substance to allow for solar heating,¹⁰ but there may not be sufficient sunlight, especially during dark winter days or periods of heavy rainfall.

Recently, the focus in fabricating new icephobic coatings has been on nature-inspired coatings. Superhydrophobic surfaces based on nanoscale features on microscale structures have been explored for achieving icephobicity.^{7–9} These surfaces are highly water repellent and have large contact angles, but their problems include (i) mechanical durability over time (the coating breaks down easily with repeated wear) and (ii) potential nucleation sites due to their microporous structures (which can result in condensate freezing). Various polymer coatings have also been explored for their anti-icing capabilities; such surfaces have promising applicability to a

wider range of surfaces and for longer-term use. For example, Kreder *et al.*¹¹ noted that various polymer coatings can be used (combining superhydrophobic surfaces with nanostructures) to lower ice adhesion. Fluorinated polymer-based coatings have also been shown to achieve low ice adhesion (of the order of 10 kPa);^{12–14} these were fabricated from polytetrafluoroethylene or polydimethylsiloxane (PDMS) elastomers cross-linked with various fluorinated polymer surfaces such as fluorinated polyhedral oligomeric silsesquioxane. The influence of PDMS-based surfaces for low ice adhesion has also been investigated, including the use of PDMS surfaces from methylated and non-methylated surfaces, lubricant-infused PDMS brush structures and cross-linked PDMS structures, PDMS-loop structures of varying chain lengths, and PDMS brushes infused with toluene vapor.^{15–18} Those investigations of the ice adhesion strength of various polymer coatings reported values in the range of 0.55–100 kPa depending on the surfaces under investigation and the slippery nature of the PDMS coatings.

Previous studies of superhydrophobic coatings often suggested that the smoother the surface, the better the performance because of the increased difficulty of ice nucleation. However, while previous studies of polymer coatings have largely been focused on altering the surfaces and coating chemistry, few studies have investigated the influences of altering a substrate's physical properties before coating with such polymer coatings regarding ice adhesion. For industrial applications, it is critical to be able to reduce ice adhesion on the rough or roughened surfaces of components.

In the study reported herein, we compared two different nanoscale hydrophobic polymer surfaces against a porous superhydrophobic coating on both glass and silicon substrates. The first polymer coating is an amorphous fluoropolymer with relatively solid/rigid but randomly orientated nanostructures, and the second is a flexible and slippery nanoscale coating formed from PDMS chains; both polymer coatings bond covalently with the surface of glass and silicon and have similar chain lengths but different physical properties. Additionally, the silicon substrates were altered physically to produce different scales of roughness to study its influences on ice adhesion. We compared the ice adhesion values of all surfaces—both glass and silicon, smooth and roughened—to those from an analytical model that estimates the ice adhesion empirically based on the receding contact angle of water on the different surfaces. Finally, we verified that after repeated ice adhesion testing, the surfaces had not been changed significantly in terms of their wettability and therefore had some robustness in terms of stability in wettability.

The substrates used in this study were glass cover slips (ca. 170 μm thick) and silicon wafers (500 μm thick) that were cleaned thoroughly before the three surface treatments of (i) hydrophobic nanoparticles (Glaco Mirror Coat; Nippon Shine), (ii) polymer treatment using amorphous fluoro chains (CYTOP; AGC Chemicals Company), and (iii) a PDMS chain structure [a so-called slippery omniphobic covalently attached liquid (SOCAL) surface]. The Glaco-coated surface represents a porous superhydrophobic nanoparticle surface, while CYTOP represents a rigid but randomly orientated polymer chain structure. The PDMS chain structures have previously been reported as having a flexible vertical arrangement that gives rise to a 4.7-nm-thick brush-like and liquid-like solid coating.¹⁹

To prepare the surfaces, the substrates first underwent a standard cleaning process consisting of sonication in a cleaning fluid solution (Decon 90) with deionized (DI) water followed by further sonication in DI water. The substrates were then cleaned with solvents consisting of acetone followed by isopropanol (IPA), and finally they were rinsed in DI water and dried with compressed air. Following the cleaning procedure, the Glaco surface²⁰ containing hydrophobic silica nanoparticles (ca. 100 nm in diameter) suspended in IPA was deposited on the various substrates; the IPA was then allowed to evaporate, leaving the particles on the structure, and this was repeated five times. The result was a superhydrophobic nanoporous structure with a thickness of ca. 1.7 μm .²⁰

The next surface treatment involved depositing a thin layer of an amorphous fluoropolymer solution (CYTOP) onto pre-cleaned substrates via dip coating to ensure an even coating across the substrate. After being dipped, the sample was placed in a tube furnace at 150 °C for 25 min, and after being cured, the obtained substrate surface was bonded covalently with the fluoropolymer chains.

The SOCAL surface was fabricated via the acid-catalyzed polycondensation of dimethyldimethoxysilane (DMDEOS), for which DMDEOS was mixed with a 98% concentration of sulfuric acid in a solution of IPA to create a liquid-like hydrophobic surface.¹⁹ Once the samples were cleaned, they were treated in a plasma oven for 30 min at a power of 30 W to create OH^- radicals on the surface. Following this step, the samples were immersed in the solution for 5 s before a slow manual withdrawal from the solution and curing in a humidity chamber at 65% relative humidity (for 20 min). This process allowed the solution to react with the exposed radicals on the surface, inducing the polycondensation of PDMS chains on the surface and creating the polymer chain structure that results in low surface energy and low contact-angle hysteresis.²¹

To form the surfaces of different roughness, silicon wafers were chosen as the substrates, and two different grades of sandpaper were used to generate different surface roughness values. The sandpaper was rubbed repeatedly over the sample for ca. 5 min, using a fabricated block to ensure that the sandpaper remained in contact with the surface and with sufficient pressure. The first grade of sandpaper chosen was P120; this was a macro grit sandpaper with a grit diameter of 162 μm , and herein after the samples roughened using this are referred to as Si P120 samples. The second grade of sandpaper chosen was P1200; this was a micro grit sandpaper with a grit diameter of 23 μm , and hereinafter the samples roughened using this are referred to as Si P1200 samples.

To characterize the wettability of the surface coatings, the contact angles (θ_{adv} for advancing and θ_{rec} for receding) and contact-angle hysteresis ($\Delta\theta$) of the various surfaces were measured using a drop shape analyzer (DSA-30; Krüss). The contact angles for the untreated, Glaco, and CYTOP surfaces were measured using an inflation–deflation procedure in which 4- μl DI water droplets were deposited on the surface before inflation and deflation of 2 μl at a flow rate of 0.5 $\mu\text{l/s}$; for the SOCAL surface, 4- μl DI water droplets were deposited on the surface before inflation by 2 μl at a flow rate of 0.033 $\mu\text{l/s}$ for 60 s and then a slow evaporation under room conditions (ca. 24 °C and ca. 40% relative humidity).

For the Glaco surface, the coating thickness was of the order of 1 μm despite being a collection of nanoparticles, and therefore a scanning electron microscopy (SEM) image was taken. However, for the two types of nanometric polymer coatings, this method is

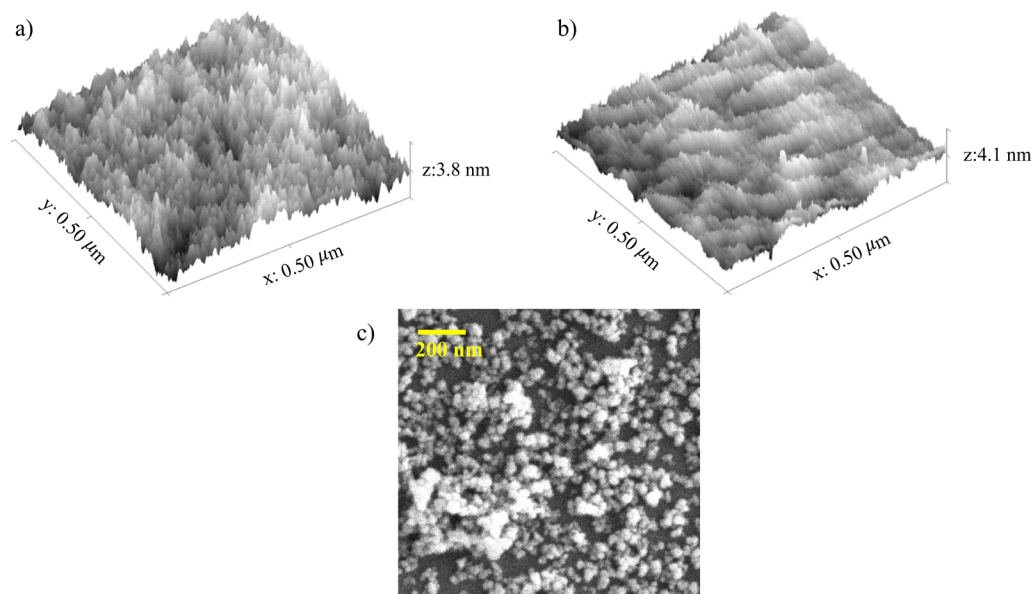


FIG. 1. (a) 3D AFM image of CYTOP surface. (b) 3D AFM image of SOCAL surface. (c) SEM image of Glaco surface.

not suitable and therefore atomic force microscopy (AFM) was used instead. To characterize the surface roughness of the Glaco coating and sanded samples, the roughness was measured using an optical profilometer (ContourGT; Bruker) within a surface area of $1.7 \text{ mm} \times 2.5 \text{ mm}$.

The ice adhesion tests were carried out using a horizontal shear force ice adhesion tester.²² Silicone molds were filled with DI water and placed on different substrates and coatings. The samples were placed in a cold chamber for 3 h for the water to freeze onto the substrate. Once the samples were frozen, they were placed in the ice adhesion testing set-up and the force required to remove the ice block was recorded.

Figures 1(a) and 1(b) show the obtained 3D profile AFM images for the CYTOP and SOCAL surfaces, and Fig. 1(c) shows an SEM image taken over a $1\text{-}\mu\text{m}$ scan at 6.0 kV to illustrate the microscale Glaco coating consisting of hydrophobic nanoparticles. From the AFM image for CYTOP, the rms roughness was 0.40 nm with an average maximum height of 2.17 nm, and the random structure of the CYTOP coating can be assumed from the absence of clear regular patterns in Fig. 1(a). By contrast, the SOCAL structure had an rms roughness of 0.75 nm with an average maximum height of 14 nm, and Fig. 1(b) shows more order to the polymer chains as seen by the distinct vertical ridges, which might indicate an ordered vertical alignment. Meanwhile, the SEM image of Glaco clearly illustrates its porous nature, with very few particles in some places and the silicon substrate visible underneath; Fig. 1(c) also illustrates the formation of clumps of nanoparticles, and this microstructure created from the hydrophobic nanoparticles gives rise to the superhydrophobicity.

Table I lists the obtained rms roughness values for the untreated glass, Glaco, and silicon samples, both untreated and roughened. The CYTOP and SOCAL values are mentioned above from the AFM

results. From the data in Table I, the Si P120 surface had the highest rms roughness, which is to be expected because it was generated with much rougher sandpaper. The Si P1200 sample had lower rms roughness, which was generated using much finer sandpaper. In both cases, the addition of the PDMS chains in SOCAL appears to have made the surface slightly smoother.

Figure 2(a) shows the differences in contact-angle measurements (θ_{adv} for advancing contact angle and θ_{rec} for receding contact angle) on the cover-slip glass substrates before and after the repeated ice adhesion testing, and Fig. 2(b) shows the contact-angle hysteresis ($\Delta\theta$, difference between θ_{adv} and θ_{rec}). For the ice adhesion results after testing, each surface underwent 15 ice adhesion tests before the contact-angle values were measured again to investigate the changes. All values in Fig. 2 are the average ones for seven repetitions on three different samples, therefore the standard deviation values were obtained. Ice adhesion results were obtained from five measurements. For the untreated glass surface, the contact angles do not appear to change significantly, but the hysteresis is decreased;

TABLE I. Measured roughness values of studied surfaces.

Surface	Rms roughness [μm]
Glass (untreated)	0.005 ± 0.002
Glass (Glaco)	0.07 ± 0.00
Si (untreated)	0.0003 ± 0.0001
Si (SOCAL)	0.00075 ± 0.0001
Si (P120, untreated)	0.19 ± 0.07
Si (P120, SOCAL)	0.12 ± 0.01
Si (P1200, untreated)	0.16 ± 0.03
Si (P1200, SOCAL)	0.14 ± 0.02

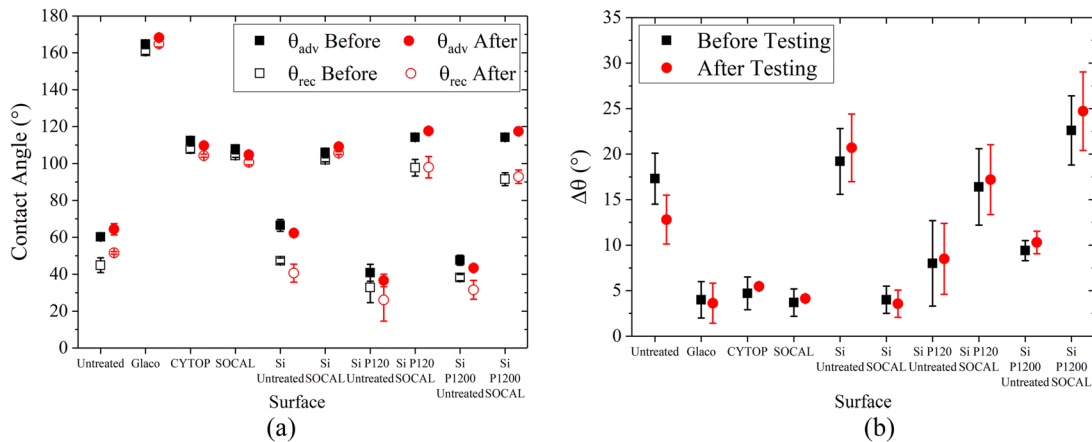


FIG. 2. Contact-angle (a) values and (b) hysteresis before and after testing for all surfaces.

this may be because of surface damage due to ice adhesion testing. For the coated glass surfaces before the adhesion testing, the contact-angle data match closely with those reported in the literature for the Glaco and SOCAL surfaces.^{20,21} For the CYTOP surface before testing, the values obtained match closely with the manufacturer's reported values. Following adhesion testing on the glass samples, there were minimal changes in θ_{adv} , θ_{rec} , and $\Delta\theta$, which shows that the coating wettability had not been changed significantly by surface damage during testing. For the roughened silicon samples, while the surface roughness was decreased by adding SOCAL, θ_{rec} was increased and $\Delta\theta$ was changed. This indicates that the morphology of the SOCAL surface is slightly different and therefore the mobility of the contact line of a droplet on the surface has been changed. This change in contact-line mobility and change in receding angle could cause increased ice adhesion. Similarly, contact-angle hysteresis has increased following ice adhesion testing in almost all cases. This may be because following repeated ice removal, the nanoscale surface structure has been disrupted by adding more scratches at the nanometric scale. However, the contact-angle data show that the wettability of the substrate is not affected significantly in the case of SOCAL.

Because the untreated glass surface was hydrophilic, a droplet on it preferentially wetted the surface. However, for the various coatings on cover-slip glass, the roughest surface was Glaco, which was mainly because of the porous nature of the coating formed of nanoparticles with 100-nm diameter; this porosity is also characterizes the superhydrophobic properties of the coating. As shown previously in the experimental results, the CYTOP coating had a lower rms roughness than the SOCAL coating, but there was a larger hysteresis due to the nature of CYTOP. The random orientation of the polymer chains results in a surface with more-variable morphology, and therefore when a droplet is undergoing inflation and deflation, there may be a nonsmooth change and so greater hysteresis. For the SOCAL coating, while it had higher rms roughness, it also had a more orientated pattern whereby more chains were vertical, as shown by the distinct lines in the AFM image. SOCAL has been shown to behave as a liquid because of the flexible

nature of the PDMS chains;¹⁵ therefore, as the droplet is inflated, there is smoother movement of the contact line, leading to lower hysteresis.

For the silicon samples, the untreated one was atomically smooth, but because of its intrinsic chemical nature, a water droplet wetted the surface and therefore the contact angle was lower than that of the SOCAL surface. When the samples were roughened, there was significant disruption to the surface in the form of increased roughness, and consequently a droplet wetted the surface further and had an even lower contact angle. Because of the morphology of the SOCAL coating, there was a lower rms roughness compared with an untreated surface. Because the PDMS chains in SOCAL are flexible and nanoscale, they follow the pattern of the microstructure. Therefore, despite the addition of the nanoscale liquid-like coating, the droplet encounters an overall rough surface. This change in the surface morphology due to the roughness affects the movement of a droplet across the surface by increasing the receding angle and the hysteresis.

When investigating the ice adhesion strength on surfaces, an analytical equation was applied in which the shear ice adhesion strength is proportional to the practical work of adhesion,¹⁵ i.e.,

$$W_p = A\gamma_w(1 + \cos\theta_{rec}), \quad (1)$$

where A is a proportionality constant, γ_w is the surface tension of a water droplet with air, and θ_{rec} is the receding contact angle. Using Eq. (1) and the receding contact angle data from Fig. 2(a), the ice adhesion strengths for a droplet of DI water on untreated cover-slip glass (22.87 kPa), Glaco (0.81 kPa), CYTOP (10.02 kPa), and SOCAL (10.08 kPa) surfaces were obtained. Given that the CYTOP and SOCAL surfaces have similar receding contact angles, their analytical values are similar. Based on Eq. (1) and the data in Fig. 2, the analytical value is highest for the untreated surface and lowest for the Glaco surface.

Figure 3 shows the differences in ice adhesion strength on the cover-slip glass among the different coatings and the untreated

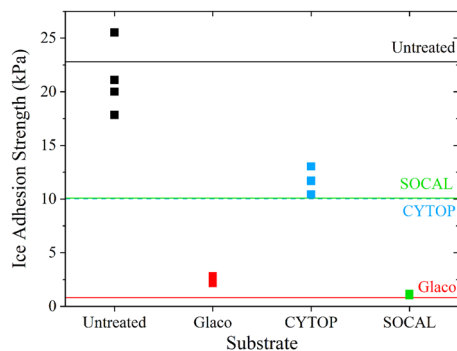


FIG. 3. Experimental data for ice adhesion on cover-slip glass compared with analytical values (black—untreated, red—Glaco, light-blue dashed—CYTOP, light-green solid—SOCAL).

sample. For each surface, four repetitions were carried out; in the case of SOCAL, the scale and the small standard deviation of the repetitions mean that these data appear as one point. Note that the experimental values for untreated, Glaco, and CYTOP lie relatively close to the analytical data (see the different lines in Fig. 3). With its superhydrophobic nature, the Glaco surface reduces the contact area of a droplet with the surface, and this reduction in contact area is linked to the high receding and advancing angles that help to reduce ice adhesion significantly. For the CYTOP surface, a droplet has a smaller contact area than on the untreated substrate but a larger contact area than on the Glaco surface; this can be seen from the surfaces' contact angles. Given that the advancing and receding contact angles for CYTOP are between those for the untreated substrate and Glaco surface, it is reasonable for the ice adhesion strength of CYTOP to be between those of the other two surfaces. However, this is not the case for the SOCAL surface because the measured ice adhesion values are much lower than the analytically predicted value. This significant change can be explained by the PDMS chains being flexible and liquid-like on the coated surfaces,¹⁵ which has been shown to remain consistent under different environmental conditions. The flexible nature of the PDMS chains means that because the block has been applied with a horizontal force, the interface between the block and the surface is easily separated, thereby reducing the adhesion of the ice block to the surface. Unlike some other types of PDMS, these chains do not detach locally because of the strong covalent bonds between the substrate and the chains. Once the block starts to move, the remaining chains covered by the block also move to aid in the removal of the ice and create the effect of a slippery surface. As a combined effect of the low surface energy of the polymeric PDMS chains with a liquid-like nature, the SOCAL surface exhibits a lower ice adhesion strength than that suggested theoretically.

We further investigated the effects of this liquid-like nature of the SOCAL coating for reducing ice adhesion on roughened surfaces. The obtained values of adhesion as a function of θ_{rec} for all glass and silicon samples are plotted in Fig. 4, where the results are fitted using Eq. (1) adjusted using a scaling factor A . All the experimental results are shown to fit using the analytically obtained values, except for the glass SOCAL surface. The ice adhesion data for Si

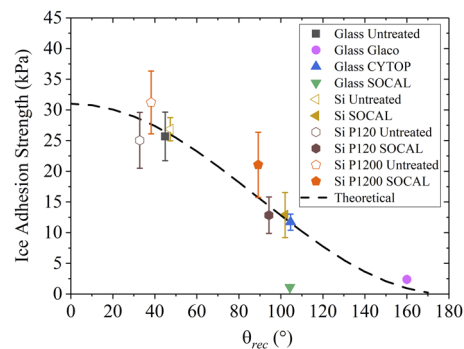


FIG. 4. Ice adhesion strength versus receding angle as determined experimentally (data points) and fitted theoretically (dashed line).

P1200 are larger than those for Si P120, smooth untreated silicon, and cover-slip glass (25.04 kPa, 26.85 kPa, and 25.67 kPa, respectively); this is because of its significantly increased ice contact area arising from the large surface roughness (Table I) from the introduction of many microscale scratches and θ_{rec} [Fig. 2(a)]. The large amount of surface features provides strong mechanical interlocking between the ice block and the substrate, resulting in a larger force required to remove the ice block. For the Si P120 surface, there are fewer but larger surface features. When the ice block is being removed from a smooth surface, the same frictional force is required to move it across the entire surface. For the Si P120 surface, there are several ridges and valleys, and once the ice is dislodged from a ridge, a valley can act as an air pocket that reduces the friction for the ice to move, therefore less force is required. The air pockets from the valleys act as breaking positions in the mechanical interlocking of the ice block with the surface.

In the case of the SOCAL surfaces, the presence of such chains decreased the ice adhesion on all the silicon samples, including the ones with increased surface roughness. The PDMS chains break the mechanical interlocking between the ice and the surface, and given their flexible nature, this reduces the force required to move the ice. Once this interlock has been broken and the first chains start to move, the rest follow, therefore reducing the ice adhesion. Given that the silicon had an ultra-smooth surface compared with the glass surface, when the surface was coated, it required more force to break the mechanical interlock and move the ice. For the Si P120 SOCAL surface and the Si P1200 SOCAL surface, the adhesion values were 12.84 kPa and 21.05 kPa, respectively; this difference in ice adhesion strength arose from differences in the surface roughness, which can also be seen through the differences in θ_{rec} and $\Delta\theta$ in Fig. 2. The Si P120 SOCAL surface had a lower rms roughness and thus a higher receding angle than those of the Si P1200 SOCAL surface; the higher receding angle then translated into a lower analytically predicted ice adhesion strength, and this is shown in the experimental data (Fig. 4).

In this work, we investigated the effects of wettability on a given substrate to reduce the ice adhesion strength of glaze ice. This investigation of the reduction in ice adhesion was realized by fabricating three different nanostructure and nanoscale coatings. We showed

that the ice adhesion of a droplet could be reduced to less than 12 kPa by using a fluoropolymer coating, then we reduced it further to less than 3 kPa by using a nanoparticle coating. We then showed that by using a nanoscale SOCAL coating, we could reduce the ice adhesion strength even more to only ca. 1 kPa. We then compared these results to a standard equation for ice adhesion and found that they matched closely with the analytical results. We investigated experimentally the influences of macroscale and microscale roughness on a selected SOCAL surface, and these results showed that for both macroscale and microscale roughness, the PDMS chain structure present in SOCAL significantly reduces the ice adhesion strength. Furthermore, we reported that even with a macroscale or microscale substrate roughness, the presence of PDMS chains on the surface lowers the ice adhesion values. The robustness of the wetting properties of all the coatings was also explored through comparisons of contact angles contact-angle hysteresis after repeated ice adhesion tests comprising ca. 15 icing/de-icing cycles.

This work was supported by the Engineering and Physical Sciences Research Council (EPSRC) of the U.K. (Grant No. EP/P018998/1), the Acoustofluidics Special Interest Group of the UK Fluids Network (Grant No. EP/N032861/1), and the EPSRC Centre for Doctoral Training in Renewable Energy Northeast Universities (ReNU) (Grant No. EP/S023836/1).

AUTHOR DECLARATIONS

Conflict of Interest

The authors have no conflicts to disclose.

DATA AVAILABILITY

The data that support the findings of this study are available from the corresponding author upon reasonable request.

REFERENCES

- ¹Frohboese P, Anders A. Effects of icing on wind turbine fatigue loads. *J Phys Conf Ser* 2007;75:012061. <https://doi.org/10.1088/1742-6596/75/1/012061>.
- ²Carriveau R, et al. Ice adhesion issues in renewable energy infrastructure. *J Adhes Sci Technol* 2012;26(4–5):447–461. <https://doi.org/10.1163/016942411x574592>.
- ³Dalili N, Edrisy A, Carriveau R. A review of surface engineering issues critical to wind turbine performance. *Renewable Sustainable Energy Rev* 2009;13(2):428–438. <https://doi.org/10.1016/j.rser.2007.11.009>.
- ⁴Gent RW, Dart NP, Cansdale JT. Aircraft icing. *Philos Trans R Soc London Ser A* 2000;358:2873. <https://doi.org/10.1098/rsta.2000.0689>.
- ⁵AAS Foundation. Safety Advisory on Aircraft Icing. 2008. pp. 1–16.
- ⁶Parent O, Ilinca A. Anti-icing and de-icing techniques for wind turbines: Critical review. *Cold Reg Sci Technol* 2011;65(1):88–96. <https://doi.org/10.1016/j.coldregions.2010.01.005>.
- ⁷Jung S, et al. Are superhydrophobic surfaces best for icephobicity?. *Langmuir* 2011;27(6):3059–3066. <https://doi.org/10.1021/la104762g>.
- ⁸Cao L, et al. Anti-icing superhydrophobic coatings. *Langmuir* 2009;25(21):12444–12448. <https://doi.org/10.1021/la902882b>.
- ⁹Farhadi S, Farzaneh M, Kulnich SA. Anti-icing performance of superhydrophobic surfaces. *Appl Surf Sci* 2011;257(14):6264–6269. <https://doi.org/10.1016/j.apsusc.2011.02.057>.
- ¹⁰Maissan JF. Wind power development in sub-arctic conditions with severe rime icing. In Proceedings of the Circumpolar Climate Change Summit. Whitehorse, Yukon, Canada: Yukon University. 2001.
- ¹¹Kreder MJ, et al. Design of anti-icing surfaces: Smooth, textured or slippery?. *Nat Rev Mater* 2016;1(1):15003. <https://doi.org/10.1038/natrevmats.2015.3>.
- ¹²Peng J, et al. Enhanced anti-icing properties of branched PDMS coatings with self-regulated surface patterns. *Sci China Technol Sci* 2020;63(6):960–970. <https://doi.org/10.1007/s11431-019-1482-x>.
- ¹³Liu B, et al. Strategies for anti-icing: Low surface energy or liquid-infused?. *RSC Adv* 2016;6(74):70251–70260. <https://doi.org/10.1039/c6ra11383d>.
- ¹⁴Zhang S, et al. Bioinspired surfaces with superwettability for anti-icing and ice-phobic application: Concept, mechanism, and design. *Small* 2017;13(48):1701867. <https://doi.org/10.1002/smll.201701867>.
- ¹⁵Zhao X, et al. Macroscopic evidence of the liquidlike nature of nanoscale polydimethylsiloxane brushes. *ACS Nano* 2021;15:13559. <https://doi.org/10.1021/acsnano.1c04386>.
- ¹⁶Sarma J, et al. Sustainable icephobicity on durable quasi-liquid surface. *Chem Eng J* 2022;431:133475. <https://doi.org/10.1016/j.cej.2021.133475>.
- ¹⁷Hao X, et al. Self-lubricative organic–inorganic hybrid coating with anti-icing and anti-waxing performances by grafting liquid-like polydimethylsiloxane. *Adv Mater Interfaces* 2022;9(18):2200160. <https://doi.org/10.1002/admi.202200160>.
- ¹⁸Li S, et al. Vapor lubrication for reducing water and ice adhesion on poly(dimethylsiloxane) brushes. *Adv Mater* 2022;34(34):2203242. <https://doi.org/10.1002/adma.202203242>.
- ¹⁹Wang L, McCarthy TJ. Covalently attached liquids: Instant omniphobic surfaces with unprecedented repellency. *Angew Chem Int Ed Engl* 2016;55(1):244–248. <https://doi.org/10.1002/anie.201509385>.
- ²⁰Geraldi NR, et al. Double-sided slippery liquid-infused porous materials using conformable mesh. *Sci Rep* 2019;9(1):13280. <https://doi.org/10.1038/s41598-019-49887-3>.
- ²¹Armstrong S, et al. Pinning-free evaporation of sessile droplets of water from solid surfaces. *Langmuir* 2019;35(8):2989–2996. <https://doi.org/10.1021/acs.langmuir.8b03849>.
- ²²Yang D, et al. Hydrophobically/oleophilically guarded powder metallurgical structures and liquid impregnation for ice mitigation. *Chem Eng J* 2022;446:137115. <https://doi.org/10.1016/j.cej.2022.137115>.



Luke Haworth is a postgraduate research student at Northumbria University in the U.K. He obtained an MPhys degree from Northumbria University in 2020, and his current postgraduate research is on anti-icing and de-icing using smart coatings and surface acoustic waves.



Deyu Yang is a postdoctoral researcher at Northwestern Polytechnical University in China. He obtained a BEng degree in metallurgical engineering from Central South University in China in 2015, an MEng degree in metallurgical engineering from the Beijing General Research Institute for Nonferrous Metals in China in 2018, and a doctoral degree in materials engineering and design from the University of Nottingham in the U.K. in 2023.



Prashant Agrawal is an assistant professor at Northumbria University. His research interests are in experimental and numerical understanding of soft matter and multi-phase fluid dynamics and its applications in healthcare diagnostics, forensics, and energy harvesting.



Hamdi Torun is an associate professor at Northumbria University. Previously, he was an associate professor at Bogazici University in Turkey. He is a cofounder of GlakoLens, a biomedical spinoff company. He received a Technology Award from the Elginkan Foundation in Turkey in 2016, a Young Scientist Award from the Science Academy in Turkey in 2016, an Innovator Under 35 Award from MIT Tech Review in 2014, and a Marie Curie Fellowship (MC-IRG Grant) in 2011. His expertise is in developing integrated micro/nanosystems especially for sensing applications.



Xianghui Hou is a professor in the School of Materials Science and Engineering at Northwestern Polytechnical University and is a Fellow of the Institute of Materials, Minerals and Mining. His current research interests include icephobic coatings, composites, and nanostructured materials.



Glen McHale is Professor of Interfacial Science & Engineering at the University of Edinburgh and a member of the Institute for Multiscale Thermo fluids. He was previously Pro-Vice-Chancellor/Executive Dean of the Faculty of Engineering & Environment at Northumbria University. He is a Fellow of the Higher Education Academy, the Institute of Physics, and the Royal Society for the Encouragement of Arts, Manufactures and Commerce, and is a Senior Member of the Institute of Electrical and Electronics Engineers. His research focuses on acoustic wave sensors, static and dynamic wetting, dielectrowetting, liquid friction, and superhydrophobic, liquid infused, and slippery liquid-like solid surfaces.



Richard YongQing Fu is a professor in the Faculty of Engineering and Environment at Northumbria University. He has extensive experience in smart thin films/materials, biomedical microdevices, energy materials, lab-on-chip, micromechanics, MEMS, nanotechnology, sensors, and microfluidics. He has published over 450 journal papers and has a Google Scholar H-index of 72 and over 22 000 citations. He is an associate editor/editorial board member for seven international journals including Nanotechnology and Precision Engineering and Scientific Reports.